ACADEMIC PRESS

Available online at www.sciencedirect.com
SCIENCE DIRECT®

Journal of Catalysis 217 (2003) 12–22

JOURNAL OF CATALYSIS

www.elsevier.com/locate/jcat

Preparation of Co–Mo/Al_2O_3 model sulfide catalysts for hydrodesulfurization and their application to the study of the effects of catalyst preparation

Yasuaki Okamoto,* Shin-ya Ishihara, Masatoshi Kawano, Masaru Satoh, and Takeshi Kubota,

Department of Material Science, Shimane University, Matsue 690-8504, Japan

Received 10 July 2002; revised 13 January 2003; accepted 23 January 2003

Abstract

The preparation conditions of a Co–Mo/Al_2O_3 model sulfide catalyst, in which CoMoS phases are selectively formed, were studied by a CVD technique using $Co(CO)_3NO$ as a precursor. The CVD technique used for the preparation of the Co–Mo/Al_2O_3 model catalyst was applied to reveal the effects of calcination and the addition of a chelating agent (NTA; nitrilotriacetic acid) on the thiophene hydrodesulfurization (HDS) activity of Co–Mo/Al_2O_3 catalysts prepared by impregnation methods. The catalysts were characterized by means of NO adsorption, TEM, FTIR, and XAFS. Al_2O_3-supported Co–Mo model catalysts were prepared by decorating presulfided Mo/Al_2O_3 with $Co(CO)_3NO$ and subsequent sulfiding. It is demonstrated that the model catalyst is prepared, when the Mo content exceeds a monolayer loading and when Mo/Al_2O_3 is calcined prior to the sulfidation. The amount of Co forming CoMoS phases was estimated from the correlation between NO/Mo and Co/Mo ratios. TEM observations have suggested that the NTA addition in the preparation of Mo/Al_2O_3 promotes the lateral growth of MoS_2 slabs. The calcination of Mo/Al_2O_3 increased the dispersion of Mo sulfide phases regardless of NTA addition. It is suggested that the NTA addition to Co–Mo/Al_2O_3 coimpregnation catalysts reduces detrimental effects of Co on the dispersion of Mo species. Furthermore, the calcination increased the Co coverage of the edge sites of MoS_2 particles on simultaneous and double impregnation catalysts. It is suggested that the present preparation technique of the model catalyst predicts the potential maximum activity of a Co–Mo catalyst under study, since the edge sites of MoS_2 particles are fully covered by CoMoS phases. In addition, the CVD technique provides a unique characterization method to evaluate the Co coverage on the edge sites of MoS_2 particles for supported Co–Mo sulfide catalysts.

Keywords: Hydrodesulfurization; Co–Mo sulfide catalyst; Model catalyst; Effects of preparation

1. Introduction

Development of highly active hydrodesulfurization (HDS) catalysts is one of the most urgent subjects in the petroleum industry not only to protect the environment but also to efficiently utilize limited natural resources. Sulfided Co–Mo or Ni–Mo(W)-based catalysts have been extensively used in industry for HDS reactions [1,2]. Numerous studies [1–10] on the catalyst systems, accordingly, have been conducted to understand the mechanism of synergy generation between Co(Ni) and Mo(W), the structure of catalytically active sites, the reaction mechanisms of HDS and hydrogenation, support effects, and so on. Since the proposal by Topsøe and co-workers [1,3,11–15], a so-called CoMoS model, in which Co decorates the edge sites of highly dispersed MoS_2 crystallites, has attracted increasing attention as catalytically active sites in Co–Mo sulfide catalysts. However, because of heterogeneity inherent to practical Co(Ni)–Mo(W) sulfide catalysts supported on refractory oxides, precise structures of active sites and HDS reaction mechanism still remain ambiguous. It is considered that understandings of the active sites of the catalysts are extensively promoted by their selective preparations. It has been found [16–21] that the addition of a chelating agent, such as nitrilotriacetic acid (NTA), in an impregnation solution provides a method to prepare selectively a Co(Ni)MoS phase, excluding the formation of separate Co(Ni) sulfide phases. The use of Co or Ni carbonyls as a precursor was reportedly effective to a preferential formation of a Co(Ni)MoS phase [22–29].

* Corresponding author.
E-mail address: yokamoto@riko.shimane-u.ac.jp (Y. Okamoto).

0021-9517/03/$ – see front matter
doi:10.1016/S0021-9517(03)00029-0

In a previous study [30], we have recently shown by XPS that Co sulfide species interacting with the preexisting MoS_2 particles are preferentially formed, when Mo sulfide catalysts supported on Al_2O_3, TiO_2, ZrO_2, or SiO_2 are exposed to a vapor of $Co(CO)_3NO$ and subsequently treated with H_2S/H_2. It has been demonstrated that the amount of Co accommodated on the Mo sulfide catalyst is proportional to the amount of NO adsorption, indicating that Co species are present on the edge sites of highly dispersed MoS_2 crystallites. In addition, the catalytic activity for thiophene HDS over the Co–Mo catalysts thus prepared was proportional to the amount of Co incorporated. On the basis of these results, we have proposed that CoMoS phases are selectively formed by use of $Co(CO)_3NO$ as a precursor and that the Co–Mo catalysts thus prepared are useful for further studies on the structure of active sites, reaction mechanism, support effect, preparation effect, and so forth. In our previous study [30], the Mo content was fixed approximately at a monolayer loading. However, $Co(CO)_3NO$ molecules adsorb on the support such as Al_2O_3 and on Co–Mo/Al_2O_3 as well as on MoS_2 particles [23,30,31]. This may pose some questions on the conditions of a selective preparation of the model catalyst system. Thus, the first purpose of the present study is to disclose the effect of Mo content of Mo/Al_2O_3 on the Co species, when $Co(CO)_3NO$ is used as a precursor.

The catalytic performance of Co–Mo sulfide catalysts depends strongly on preparation variables and additives [1,2]. The preparation method may modify the edge dispersion and stacking degree of MoS_2 particles and the efficiency of transformation of Co to CoMoS phases. In the present study, by use of the preparation technique of the model catalysts we studied the effects of NTA addition, calcination, and Co precursor salt with respect to Co–Mo/Al_2O_3 catalysts prepared by a conventional impregnation technique. Finally, it is suggested that the model catalyst preparation technique can be used to assess the potential maximum HDS activity of a Co–Mo sulfide catalyst under study.

2. Experimental

2.1. Catalyst preparation

Al_2O_3-supported Mo oxide catalysts having 3.4–22.2 wt% Mo were prepared by an impregnation technique using $(NH_4)_6Mo_7O_{24} \cdot 4H_2O$ (Kanto Chemicals, analytical grade). After evaporation of the impregnation solution to dryness at ca. 350 K while stirring, the catalyst was dried at 383 K for 16 h. Calcination was carried out in air at 773 K for 5 h by using an electric furnace. Al_2O_3 (JRC-ALO-4: 177 $m^2\,g^{-1}$) used for the study of the effect of Mo loading was supplied by the Catalysis Society of Japan as the Reference Catalysts. MoO_3/Al_2O_3 catalysts (9.1 wt% Mo) were also prepared to examine the effects of calcination and NTA addition (NTA/Mo mole ratio 1.2).

A series of Co–Mo/Al_2O_3 catalysts (9.1 wt% Mo, 2.0 wt% Co, Co/Mo = 0.36) was prepared by a simultaneous impregnation technique using $(NH_4)_6Mo_7O_{24} \cdot 4H_2O$ and $Co(CH_3COO)_2 \cdot 4H_2O$ (Kanto Chemicals, analytical grade) in the presence and absence of NTA (NTA/Mo mole ratio 1.2), followed by drying at 383 K for 16 h. The pH of the solution was not adjusted. JRC-ALO-4 Al_2O_3 was used as a support. An aliquot of the catalyst was calcined at 773 K for 5 h.

Another series of Co–Mo/Al_2O_3 catalysts (9.1 wt% Mo, 2.7 wt% Co, Co/Mo = 0.48) was prepared by impregnating a calcined MoO_3/Al_2O_3 (Al_2O_3: JRC-ALO-6, 180 $m^2\,g^{-1}$) with an aqueous solution of $Co(CH_3COO)_2$ or $Co(NO_3)_2$, followed by drying at 383 K for 16 h. An aliquot of the catalyst was calcined at 773 K for 5 h.

The Mo or Co–Mo catalyst (0.1 g) was sulfided in a 10% H_2S/H_2 flow (100 $cm^3\,min^{-1}$). The sulfidation temperature was raised from room temperature to 373 K at a rate of 2 K min^{-1} and kept isothermal at 373 K for 1 h. Subsequently, the temperature was ramped to 673 K at a rate of 5 K min^{-1} and then kept at 673 K for 1.5 h. After the sulfidation, the sample was cooled in the H_2S/H_2 stream to room temperature to prepare a sulfide catalyst. The Mo sulfide catalyst is designated Mo/Al here with Mo content in parentheses when necessary. Mo/Al prepared using NTA is denoted Mo/Al(NTA). The Co–Mo sulfide catalysts prepared by the coimpregnation and double impregnation techniques are denoted CoMo/Al for simplicity. The sulfide catalysts prepared from the calcined and uncalcined precursor are shown such as Mo/Al(calc.) or Mo/Al(uncalc., NTA), when necessary.

A chemical vapor deposition (CVD) technique was used to introduce Co to the sulfided catalysts. Mo/Al or CoMo/Al was evacuated at 673 K for 1 h ($< 1 \times 10^{-3}$ Pa) prior to exposure to a vapor of $Co(CO)_3NO$ (Strem Chemicals) at room temperature [30]. A vapor pressure of $Co(CO)_3NO$ at 290–300 K (room temperature) was used. After a 5-min exposure, the sample was evacuated at room temperature for 10 min to remove physisorbed $Co(CO)_3NO$ molecules. The exposure time was chosen at 5 min, since the HDS activity and Co content were not varied within the accuracies when the exposure time was longer than 1 min under the present conditions. The sample was subjected again to the same temperature-programmed sulfidation in a 10% H_2S/H_2 stream as described above to produce a Co–Mo sulfide catalyst, unless otherwise stated. The catalyst prepared using $Co(CO)_3NO$ is denoted CVD-Co/Mo/Al (Mo/Al was used) or CVD-Co/CoMo/Al (CoMo/Al was modified). A supported Co sulfide catalyst (CVD-Co/Al) was prepared by exposing presulfided Al_2O_3 to a $Co(CO)_3NO$ vapor. The other procedures were identical to those with CVD-Co/Mo/Al. The Co content anchored by the CVD technique was determined for the sulfided catalysts by means of XRF (Rigaku RIX 2000).

2.2. Reaction procedure

The catalyst sulfided in situ (0.1 g) was evacuated at 673 K for 1 h before catalytic reaction. In order to evaluate the initial activity of the freshly prepared catalyst, the reaction was conducted under mild conditions using a circulation system (200 cm^3) made of glass [26–30]. The HDS of thiophene was carried out at 623 K and the initial H_2 pressure of 20 kPa. The thiophene pressure was kept constant (2.6 kPa) during the reaction by holding a small amount of liquid thiophene kept at 273 K as a reservoir in the bottom of a U-shaped tube in the circulation system. The reaction products were analyzed by on-line gas chromatography. The products were mainly C_4 compounds and a corresponding amount of H_2S. The amount of H_2S formation was periodically monitored during the reaction. The HDS activity was calculated on the basis of the accumulated amount of H_2S evolved after 1 h. The amounts of H_2S evolution from the sulfided catalysts were estimated by blank experiments without introduction of thiophene vapor into the reactor, showing that they were negligibly small ($< 5–10 \times 10^{-5}$ mol h^{-1} g^{-1}) compared with the amounts of H_2S formed by the HDS reaction.

2.3. Characterization

2.3.1. NO adsorption

The amount of NO adsorption on Mo/Al was measured by a pulse technique [30]. After cooling in the H_2S/H_2 stream, the sulfided catalyst (0.1 g) was flushed at room temperature with a high-purity He stream (20 cm^3 min^{-1}). A pulse of 5.0 cm^3 of 10% NO/He (purity of NO: $> 99\%$, atmospheric pressure) was repeatedly injected every 8 min to the He stream by using a six-way stopcock until no adsorption was detected (pulse size; 20 μmol NO/pulse, 15–20 pulses). The effluent gas was analyzed by a gas chromatograph equipped with a thermal conductivity detector to measure the amount of NO. The amount of NO adsorption was calculated from the cumulative amount of NO adsorption. The reproducibility was usually better than ±5% of the total amount of NO adsorption.

2.3.2. XAFS measurements

Mo K-edge XAFS spectra for Mo/Al and reference compounds were measured in a transmission mode at room temperature at BL-10B in the Photon Factory of Institute of Materials Structure Science, High Energy Accelerator Research Organization (KEK-IMSS-PF), with 2.5 GeV ring energy and 250–290 mA stored current [29]. The synchrotron radiation was monochromatized by a Si (311) channel-cut monochromator. The number of scans was three for each sample and the sum spectrum was used for further analysis. The EXAFS data were analyzed assuming a spherical wave approximation and a single scattering model. The EXAFS data were Fourier-transformed from k-space (40–150 nm^{-1}) to R-space. The empirical backscattering amplitude and phase shift for Mo–S and Mo–Mo pairs were extracted from the EXAFS data for polycrystalline MoS_2.

2.3.3. IR measurements

The FTIR spectra of Al_2O_3 were recorded in a transmission mode at room temperature on a single-beam FTIR spectrophotometer (JASCO, FTIR-620V). The resolution of the spectrometer was set at 2 cm^{-1}). A self-supporting wafer of Al_2O_3 (ALO-4) was evacuated in an in situ IR cell at 773 K for 1 h ($< 1 \times 10^{-3}$ Pa). After the sample was cooled to room temperature, the IR spectra were measured and background spectrum was subtracted. Subsequently, the Al_2O_3 wafer was exposed to a vapor of $Co(CO)_3NO$ for 1 min, followed by evacuation for 10 min. The IR spectra of the sample were recorded again.

2.3.4. TEM observations

Transmission electron microscopic (TEM) images of Mo/Al were taken on an electron microscope JEM-2010 (JEM) with an accelerating voltage of 200 keV [32]. The Mo/Al powder sample was evacuated and sealed in a glass tube without exposure to air. The catalyst sample was suspended in acetone and placed on a specimen grid in a glove-bag filled with N_2 gas to avoid as much contact with air as possible. The sample was then transferred in a stream of N_2 to a sample holder attached to the microscope. The distributions of MoS_2 particle size and stacking were calculated over ca. 300 particles in two or three arbitrary chosen areas.

3. Results and discussion

3.1. Effects of Mo loading on the distribution of Co species

Fig. 1A shows the thiophene HDS activities of Mo/Al and CVD-Co/Mo/Al as a function of Mo content. The maximum activity of Mo/Al was attained around 10–15 wt% Mo in agreement with a previous study [33]. According to the literature [34–37], it is considered that in the present series of Mo/Al, a monolayer dispersion of Mo is attained around 8.5 wt% Mo (3 Mo nm^{-2}). The addition of Co by the CVD technique greatly enhanced the HDS activity. The activity of CVD-Co/Mo/Al is not very dependent on the Mo content between 6.9 and 22.2 wt% Mo with a maximum being observed around 14 wt% Mo. The increase in the activity by the addition of Co, (activity of CVD-Co/Mo/Al)/(activity of Mo/Al), depended on the Mo content and was relatively high at a Mo content below 6.9 wt% Mo as shown in Fig. 1B.

As noted above, it has been shown [30] that when the Mo content corresponds to a monolayer loading, a CoMoS phase is selectively formed on supported MoS_2 catalysts by using $Co(CO)_3NO$ as a Co precursor. Fig. 2 shows the amount of Co accommodated on Mo/Al as a function of Mo content. It should be noted that a considerable amount of Co is

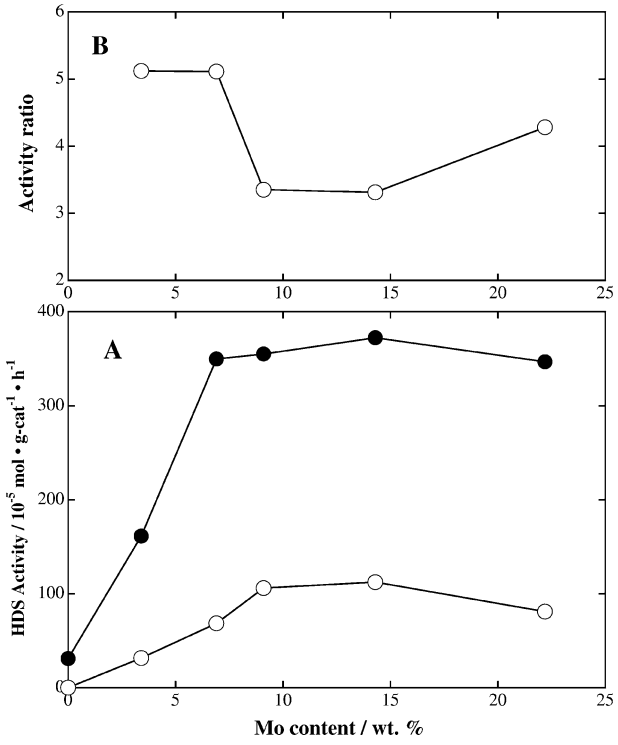

Fig. 1. (A) HDS activities of Mo/Al (○) and CVD-Co/Mo/Al (●) as a function of Mo content. (B) Activity ratio of CVD-Co/Mo/Al to Mo/Al as a function of Mo content.

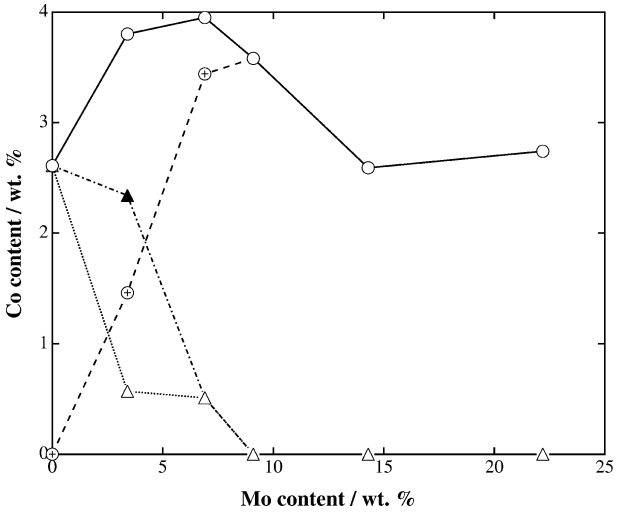

Fig. 2. The amount of Co species in CVD-Co/Mo/Al as a function of Mo content. ○, The total amount of Co accommodated by the CVD technique; △, the amount of Co sulfide clusters produced by the interaction with basic sites of Al_2O_3; ▲, the total amount of separate Co sulfide clusters; and ⊕, the amount of Co species forming CoMoS phases.

loaded even when the support Al_2O_3 is exposed to a vapor of $Co(CO)_3NO$. The amount of Co increased as the Mo content increased to 6.9 wt%. After taking a maximum at 6.9 wt% Mo, the Co content decreased on a further increase in Mo loading and leveled off at a Mo content higher than 14 wt%. In conformity with this, Okamoto et al. [26] reported that the accommodation amount of Co was increased by the addition

Table 1
Amount of NO adsorption of Mo/Al[a] and the Co content of CVD-Co/Mo/Al

Mo content (wt%)	NO/Mo (mol mol^{-1})	Co content (wt%)	Co/Mo atomic ratio
0	–	2.61	–
3.4	0.480	3.80	1.81
6.9	0.265	3.95	0.93
9.1	0.202	3.58	0.64
14.3	0.104	2.59	0.29
22.2	0.063	2.74	0.20

[a] Al_2O_3, JRC-ALO-4.

Table 2
Structural parameters[a] as derived from the Mo K-edge EXAFS for sulfided Mo/Al_2O_3 catalysts (Mo/Al)

Mo content (wt%)	Absorber–scatterer pair	R (nm)	CN	E_0 (eV)	σ (nm)	R_f (%)
3.4	Mo–S	0.240	4.1	−0.7	0.0072	1.6
	Mo–Mo	0.315	2.0	1.6	0.0077	
6.9	Mo–S	0.241	5.1	0.7	0.0067	0.7
	Mo–Mo	0.315	2.6	1.6	0.0066	
9.1	Mo–S	0.241	4.7	−0.5	0.0066	0.8
	Mo–Mo	0.316	2.9	1.1	0.0072	
14.3	Mo–S	0.241	4.8	−0.1	0.0066	0.9
	Mo–Mo	0.315	2.9	0.5	0.0069	
Reference compound						
MoS_2	Mo–S	0.241	6.0	0.00	0.0060	
	Mo–Mo	0.361	6.0	0.00	0.0060	

[a] R, distance; CN, coordination number E_0, inner potential σ, Debye–Waller-like factor; R_f, R factor defined as $R_f = \{\sum[\chi_{obs}(k) - \chi_{cal}(k)]^2 / \sum \chi_{obs}(k)^2\}^{1/2}$.

of Mo to Al_2O_3 when $Co_2(CO)_8$ was used as a precursor. These results suggest the interactions of Mo sulfide species and $Co(CO)_3NO$ molecules.

The amount of NO adsorption was measured for Mo/Al to assess the dispersion degree of Mo sulfides. They are presented in Table 1. The NO/Mo ratio decreased as the Mo content increased, indicating that the dispersion of Mo sulfides decreases with increasing Mo loading. The dispersion of Mo sulfides was also examined by EXAFS. Table 2 summarizes the structural parameters for Mo/Al. The Mo–S and Mo–Mo atomic distances were in conformity with those for crystalline MoS_2. The coordination number of the Mo–Mo contribution increased as the Mo content increased to 9.1 wt% Mo and leveled off at $>$ 9.1 wt%. It is evident that the EXAFS technique is not as sensitive as the NO adsorption method for the evaluation of the Mo sulfide dispersion. This obviously results from the fact that EXAFS information is limited to the local structure of Mo atoms averaged over the whole Mo sulfide phases.

In our previous study [30], it has been shown that the amount of Co (Co/Mo) thus accommodated is proportional to the NO adsorption capacity (NO/Mo) for a series of monolayer MoS_2 catalysts. On the basis of the finding, we have proposed that the Co atoms introduced to Mo/Al decorate the edge sites of MoS_2 particles to form Co–MoS_2 in-

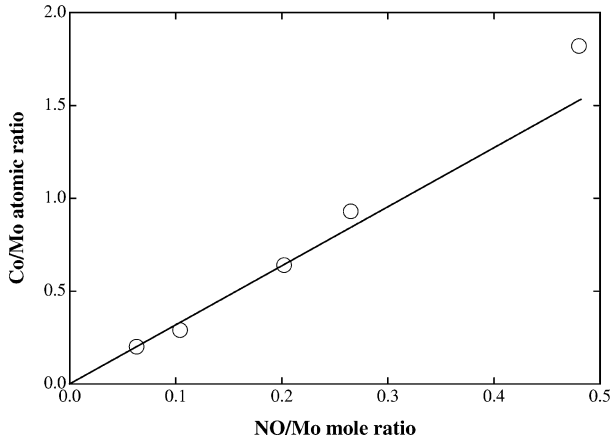

Fig. 3. Correlation between the NO/Mo mole ratio for Mo/Al and the Co/Mo atomic ratio for CVD-Co/Mo/Al.

teraction species, i.e., CoMoS phases, since it is well established [1] that NO molecules adsorb on coordinatively unsaturated Mo sites on the edge sites of MoS_2 particles. It has been shown by XPS and HDS activity measurements [30] that no additional Co is incorporated on the edge sites of MoS_2 particles. In order to examine whether Co species interact with the Mo sulfides in the present series of CVD-Co/Mo/Al, the Co/Mo atomic ratio is plotted in Fig. 3 against the NO/Mo mole ratio. With Mo/Al ($\geqslant$ 9.1 wt%), the Co/Mo ratio was proportional to the NO/Mo ratio. The slope of the linear line in Fig. 3 is in excellent agreement with that reported previously [30] for supported MoS_2 catalysts with a monolayer loading of Mo, demonstrating that the Co species in these catalysts interact selectively with the edge sites of MoS_2 particles. On the other hand, when the Mo content was below the monolayer loading ($<$ 9.1 wt%), the Co/Mo ratio was higher than the value expected from the linear line. Fig. 3 suggests that an excess amount of Co over that required for full decoration of MoS_2 edge sites is anchored when Mo/Al has a Mo content less than the monolayer loading. Taking into consideration the finding that Co sulfide clusters are anchored on Al_2O_3 by using $Co(CO)_3NO$ as a precursor (Fig. 1), it is considered that the excess Co is located on bare Al_2O_3 sites, when the Mo content is below the monolayer. The amount of Co sulfides adsorbed on Al_2O_3 was calculated by assuming that the amount of the Co species interacting with the MoS_2 particles was provided by the linear correlation in Fig. 3. The amount of Co sulfide clusters on Al_2O_3 thus estimated is shown in Fig. 2 as a function of Mo content. It decreases sharply on the addition of a small amount of Mo, 3.4 wt%, and disappears at 9.1 wt% Mo, the monolayer loading.

With MoO_3/Al_2O_3, it is well established [34–37] that Mo oxide species in tetrahedral configurations (Mo_{tet}) are predominantly formed below the Mo content of 0.7–0.9 Mo nm^{-2} (2–2.5 wt% Mo in the present Mo/Al) at the expense of basic hydroxyl groups on the Al_2O_3 surface. The maximum amount of Mo_{tet} species was estimated to be 1.7 Mo nm^{-2} and close to the number of the most basic hydroxyl

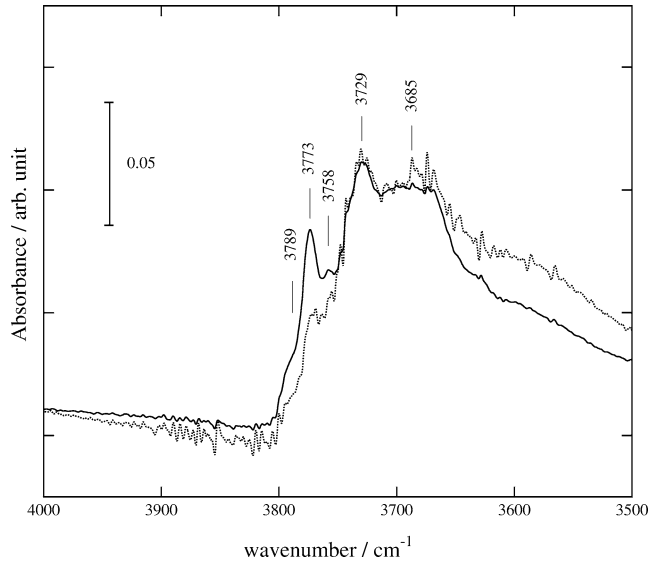

Fig. 4. FTIR spectra of the hydroxyl groups of Al_2O_3. Solid line, after evacuation at 773 K; and dotted line, after adsorption of $Co(CO)_3NO$.

groups [37]. The formation of polymolybdate species is detected at 1.3–1.5 Mo nm^{-2} (3.5–4.1 wt% Mo). A monolayer of Mo oxides is usually established around 3 Mo nm^{-2} (8.5 wt% Mo). It is considered that a sharp decrease in the amount of Co sulfide clusters by the addition of 3.4 wt% Mo (Fig. 2) is caused by the consumption of the basic hydroxyl groups by the loading of Mo, with which $Co(CO)_3NO$ molecules also strongly interact as substantiated by the FTIR results in Fig. 4, where the FTIR spectra of the surface hydroxyl groups of the Al_2O_3 sample are compared before and after $Co(CO)_3NO$ adsorption. It is well known that the bands at 3789 and 3773 cm^{-1} are basic in nature [35–38]. It is apparent that these bands are significantly reduced in intensity by the introduction of $Co(CO)_3NO$, while the hydroxyl bands observed below ca. 3730 cm^{-1} (neutral or weakly acidic) are not affected. This substantiates selective interactions of $Co(CO)_3NO$ with the basic hydroxyl groups of Al_2O_3 as observed for Mo oxide species [35–37]. The amount of $Co(CO)_3NO$ adsorbed on Al_2O_3 is 2.61 wt% Co or 1.5 Co nm^{-2} and is close to the maximum amount of Mo_{tet} species on Al_2O_3 [37].

In our previous study [30], it has been demonstrated that the HDS activity of CVD-Co/Mo/support is proportional to the amount of Co for the monolayer catalysts. Fig. 5 shows the HDS activity of CVD-Co/Mo/Al having a variety of Mo content as a function of Co content. The activities of the supported CVD-Co/Mo catalysts having the monolayer loadings of Mo [30] are also presented, for comparison. It has been proposed [30] that the solid line in Fig. 5 represents the activity of CoMoS(I) (Co–Mo–S Type I [1]), while the dotted line that of CoMoS(II) (Co–Mo–S Type II [1]). The turnover frequency (the slope of the line) of thiophene HDS on CoMoS(II) is 1.7 times higher than that on CoMoS(I) in agreement with other workers [15,18]. With CVD-Co/Mo/Al exceeding a monolayer loading of

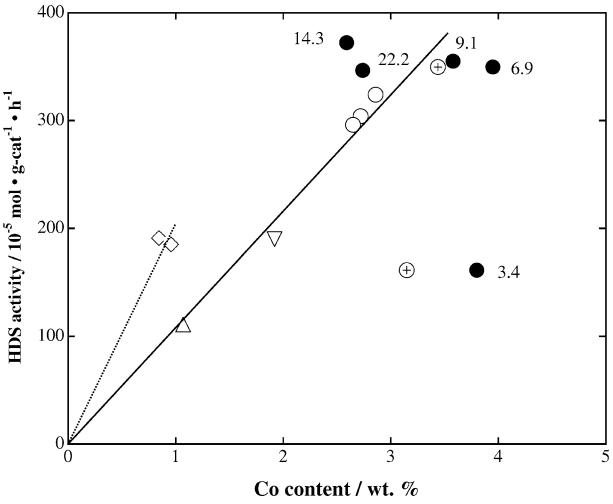

Fig. 5. HDS activity of CVD-Co/Mo/Al as a function of Co content. Some previous results [30] are also presented for comparison. ●, CVD-Co/Mo/Al (Mo content is shown in the figure); ⊕, CVD-Co/Mo/Al corrected for the Co content of Co_9S_8 clusters; ○, CVD-Co/Mo/Al_2O_3 [30]; ▽, CVD-Co/Mo/TiO_2 [30]; △, CVD-Co/Mo/ZrO_2 [30]; ◇, CVD-Co/Mo/SiO_2 [30].

Mo (14.3 and 22.2 wt% Mo), the activity was higher than that expected from the linear line for CoMoS(I), suggesting a partial formation of CoMoS(II) possibly due to increased stacking degree of MoS_2 slabs at high Mo content [15,18,30]. With the monolayer catalyst (9.1 wt% Mo), the activity is close to that expected for CoMoS(I). On the other hand, CVD-Co/Mo/Al catalysts having lower Mo contents showed considerably lower activities than those expected from the Co contents. It is considered that the low activities of these catalysts are attributed to simultaneous formations of a CoMoS phase and Co sulfide clusters, the latter exhibiting a much less activity for HDS. The amount of the CoMoS phase was estimated from the linear line in Fig. 3 as described above. The activities are plotted for the catalysts with 3.4 and 6.9 wt% Mo by using the estimated amount of the CoMoS phase. Obviously, the activity of CVD-Co/Mo/Al(6.9) became well correlated to the activity of CoMoS(I) as shown in Fig. 5. However, the activity of CVD-Co/Mo/Al(3.4) was still far below that expected for CoMoS(I) even after the correction, suggesting a lower content of CoMoS(I) or lower specific activity of Co–Mo interaction species in the catalyst. As discussed above, it has been shown by a variety of techniques [34–37,39] that Mo oxide species in tetrahedral configurations predominate in MoO_3/Al_2O_3 at a low Mo content (< 2.5 wt% Mo) and that these Mo oxide species are not easily sulfided to MoS_2 particles but tend to transform to isolated or small clusters of Mo oxysulfides. The relatively low coordination number of Mo–S bondings for Mo/Al(3.4) (Table 2) may be explained in terms of the formation of these species. It is proposed here that $Co(CO)_3NO$ molecules are anchored on these oxysulfide species, which also adsorb NO molecules, to form separate Co sulfide clusters on the subsequent sulfidation. The fraction of Co to form CoMoS(I) in CVD-Co/Mo/Al(3.4) is estimated to be about 40% of the total amount of Co from the activity–Co content correlation in Fig. 5. Fig. 2 shows the amounts of CoMoS phases and Co sulfide clusters thus estimated as a function of Mo content.

It has been proposed previously [30] that the adsorption sites of $Co(CO)_3NO$ on Mo sulfide species are coordinatively unsaturated sulfur anions. It has been demonstrated [30] that when CVD-Co/Mo/Al is exposed to a vapor of $Co(CO)_3NO$ again, the additional $Co(CO)_3NO$ molecules are transformed to only Co sulfide clusters without further formation of CoMoS phases. Taking into account these results, the fate of $Co(CO)_3NO$ molecules adsorbed on Mo/Al and CoMo/Al is schematically presented in Fig. 6. It is concluded that the primary conditions of selective preparation of CoMoS phases by use of $Co(CO)_3NO$ are to use a supported MoS_2 catalyst (calcined, vide infra) having a Mo content higher than a monolayer loading. At the monolayer loading, the basic OH groups are completely consumed by the reaction with the Mo phase and oxysulfide species are sulfided to MoS_2 and/or involved in MoS_2 particles as anchoring sites to Al_2O_3. A single exposure to a vapor of $Co(CO)_3NO$ (e.g., 5 min at room temperature) was suffi-

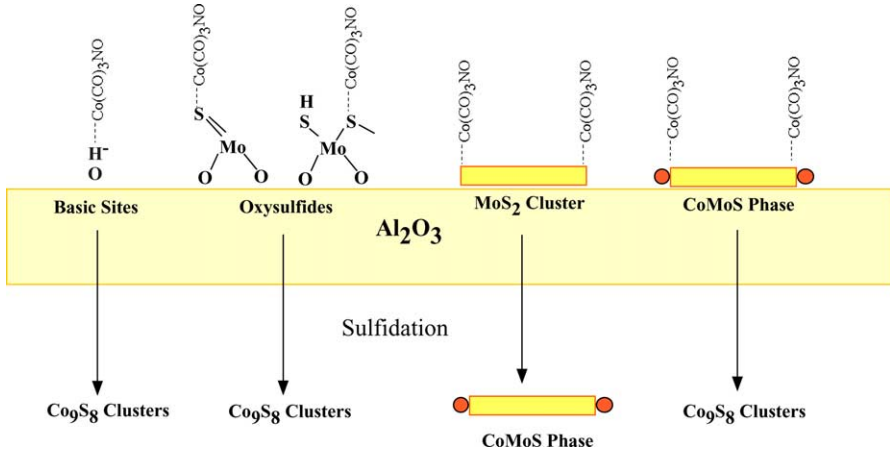

Fig. 6. Schematic model showing the fate of adsorbed $Co(CO)_3NO$ molecules on the sulfidation.

cient to prepare the maximum amount of CoMoS phases. CVD-Co/Mo/Al catalysts ($\geqslant 9.1$ wt% Mo) thus prepared are regarded as Co–Mo model catalysts, since the Co species are present only as CoMoS phases. It is considered that the model catalyst systems can be used for the study of active sites structure and reaction mechanism because of their simplicity. The effects of support have been studied by using the model Co–Mo catalysts and reported elsewhere [30].

It is worthy of note that the slope of the line in Fig. 3 indicates an adsorption stoichiometry of Co/NO = 3. Taking into consideration the adsorption form of NO (dinitrosyl [40,41]) on Mo sulfide species, the slope of the proportional line in Fig. 3 suggests that the amount of Co atoms which form CoMoS phases is about six times larger than the amount of NO adsorption sites or coordinatively unsaturated (cus) Mo sites. This fact indicates that NO molecules and Co sulfide species are anchored on different MoS_2 edge sites, the former on cus Mo sites, while the latter cus sulfur sites as suggested previously [30]. A considerably high Co/Mo atomic ratio (e.g., 0.64 for the monolayer catalyst, 9.1 wt%) suggests that the edge sites of MoS_2 particles are fully covered by Co species forming CoMoS phases. In contrast, the fraction of cus Mo sites accessible to NO adsorption is considerably small under the present adsorption conditions.

3.2. Effects of calcination and NTA addition on the preparation of Mo/Al_2O_3

The preparation technique of the model catalysts was applied to disclose the effects of calcination and NTA addition on the catalytic performance of supported Co–Mo sulfide catalysts. First of all, we studied their effects on the preparation of Mo/Al(9.1). Table 3 summarizes the NO/Mo mole ratio to assess the edge dispersion of MoS_2 particles. It is evident that the edge dispersion of MoS_2 particles is increased by the calcination at 773 K for Mo/Al regardless of NTA addition, whereas it is decreased by the addition of NTA.

The size and stacking degree of MoS_2 particles were observed by means of TEM for the catalysts in Table 3. The distributions of stacking number and slab length are presented in Figs. 7 and 8, respectively. Small but significant changes were observed with the preparations. With the stacking number of MoS_2 slabs, the NTA addition rather favored single slab MoS_2 particles in the present preparations. The forma-

Table 3
Effects of calcination and NTA addition on the HDS activity of CVD-Co/Mo/Al[a]

Preparation[b]	NO/Mo	Activity[c] of CVD-Co/Mo/Al	Co content[d] (wt%)	Co/Mo[d]
Uncalc.	0.169	314	3.99 (3.03)	0.71 (0.54)
Calc.	0.202	355	3.56	0.64
Uncalc. + NTA	0.154	320	4.16 (2.72)	0.74 (0.48)
Calc. + NTA	0.175	356	3.07	0.55

[a] Mo content, 9.1 wt%; Al_2O_3, JRC-ALO-4.
[b] Calc., calcined at 773 K and uncalc., dried but not calcined.
[c] 10^{-5} mol g^{-1} h^{-1}.
[d] The Co content in parentheses is that forming CoMoS phases.

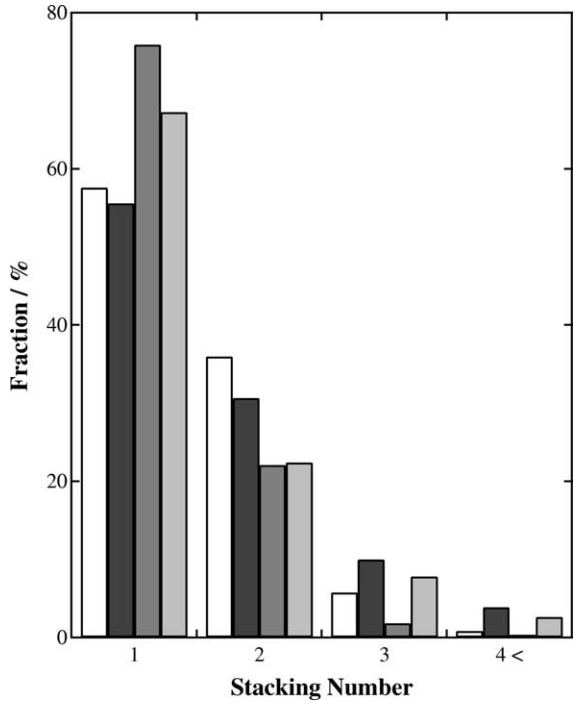

Fig. 7. The distribution of stacking number of MoS_2 particles as observed by TEM. White bar, Mo/Al(calc.); black bar, Mo/Al(uncalc.); dark gray bar, Mo/Al (calc., NTA); and light gray bar, Mo/Al(uncalc., NTA).

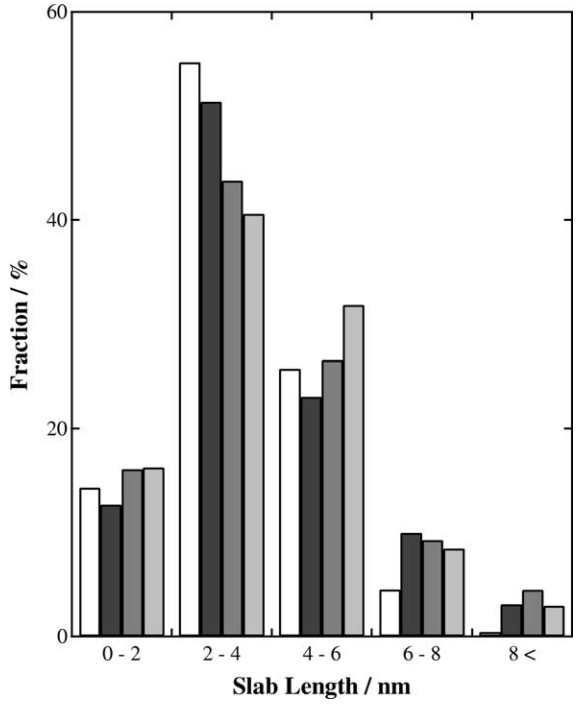

Fig. 8. The distribution of slab length of MoS_2 particles as observed by TEM. White bar, Mo/Al(calc.); black bar, Mo/Al(uncalc.); dark gray bar, Mo/Al (calc., NTA); and light gray bar, Mo/Al(uncalc., NTA).

tion of highly stacked MoS_2 particles ($\geqslant 3$ layers) was observed for the uncalcined Mo/Al. With the size of MoS_2 particles, the most abundant slab length was in the range of 2–4 nm for all the catalysts. However, it appears that the calcination decreases the size of MoS_2 particles, while NTA addition increases it, in conformity with the tendencies observed for the NO adsorption.

In order to obtain a semiquantitative correlation about the edge dispersion of MoS_2 particles between NO adsorption and TEM observations, a parameter α is proposed for anisotropic structure of MoS_2,

$$\alpha = \sum_{n=1}\sum_{i} n d_{n,i} \Big/ \sum_{n=1}\sum_{i} n d_{n,i}^2, \tag{1}$$

where n and $d_{n,i}$ represent the stacking number and length of particle i, respectively. The numerator is proportional to the total number of edge sites and the denominator to the total volume of MoS_2 particles, assuming that the MoS_2 particles have similar geometries, such as hexagon. The parameter α is plotted in Fig. 9 as a function of the NO/Mo mole ratio. A good proportional correlation suggests that the size and stacking distributions of MoS_2 particles observed by the present TEM technique represent their morphology and that the edge dispersion of MoS_2 particles are reasonably estimated both by the NO adsorption and TEM observations. It will be safe to say that parameter α is simple but useful for a similar series of catalysts. Payen et al. [42] presented a more rigorous correlation to estimate the dispersion of MoS_2 particles by using TEM.

The HDS activity and Co content of CVD-Co/Mo/Al are also presented in Table 3. The apparent activity of the calcined catalyst was unaffected by the NTA addition and higher than that of the uncalcined catalyst. The amount of Co of CVD-Co/Mo/Al(uncalc.) was much larger than that of the calcined counterpart. In order to determine the amount of Co forming CoMoS phases, the Co/Mo ratio is plotted in Fig. 10 against the NO/Mo ratio. The results in Fig. 3 for CVD-Co/Mo/Al(14.2 and 22.2) are also included in Fig. 10, for comparison. The calcined catalyst without NTA addition is the same catalyst as Mo/Al(9.1) in Fig. 3. Obviously, irrespective of the addition of NTA, the Co/Mo ratio for the calcined catalysts was well correlated to the line for selective formation of CoMoS phases. It is, accordingly, concluded that Co is selectively located on the edge sites of MoS_2 particles for the calcined catalysts. However, the uncalcined catalysts showed the Co/Mo ratio much higher than those expected from the edge dispersion of MoS_2 particles. It is considered that the excess Co is produced by the adsorption of $Co(CO)_3NO$ on the basic sites of the bare Al_2O_3 surface. The amount of Co forming CoMoS phases was estimated from the proportional line in Fig. 10 as discussed above and is presented in Table 3. It is thus estimated that about 25 and 35% of the total incorporated Co are present as Co sulfide clusters in CVD-Co/Mo/Al(uncalc.) in the absence and presence of NTA, respectively. It is considered that reactions between surface basic hydroxyl groups and Mo oxide species take place to completeness only during calcination processes at high temperature and, accordingly, that calcination of MoO_3/Al_2O_3 at high temperature is a necessary process for the preparation of the Co–Mo model catalysts using $Co(CO)_3NO$. It is considered that the presence of NTA considerably prevents the Mo anion–Al_2O_3 reactions to occur due to decreased pH of the impregnation solution (pH, 1–2) [35,36] and, in part, to complex formations with Mo anions [43,44].

Fig. 11 shows the HDS activity of CVD-Co/Mo/Al(9.1) in Table 3 as a function of Co content. The HDS activities of CVD-Co/Mo/support reported previously [30] are also included in Fig. 11, for comparison. While the activity of CVD-Co/Mo/Al(calc.) without NTA addition was close to the correlation confirming a selective formation of CoMoS(I), the activities of CVD-Co/Mo/Al(uncalc.)

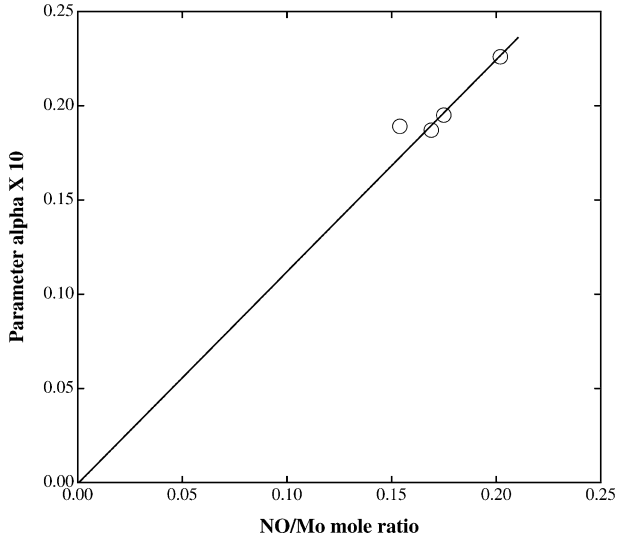

Fig. 9. Correlation between the parameter α and NO/Mo mole ratio.

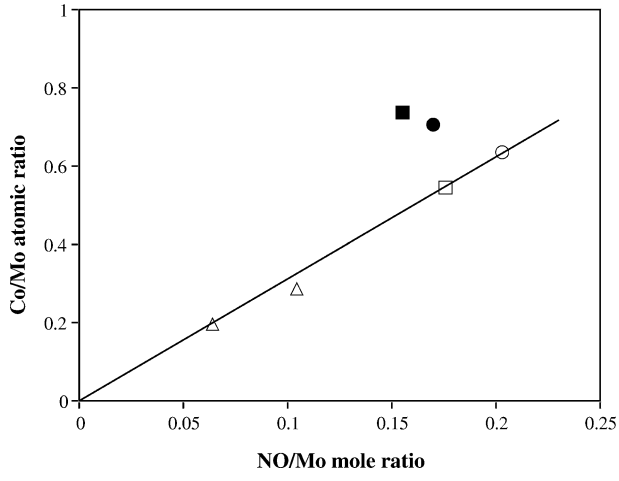

Fig. 10. Correlation between the NO/Mo mole ratio for Mo/Al(9.1) and the Co/Mo atomic ratio for CVD-Co/Mo/Al. ○, Mo/Al(calc.); □, Mo/Al (calc., NTA); ●, Mo/Al(uncalc.); ■, Mo/Al(uncalc., NTA); and △, Mo/Al having 14.3 and 22.2 wt% Mo in Fig. 3.

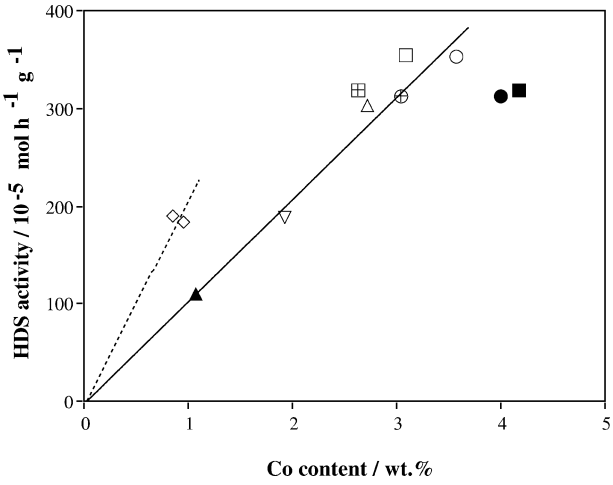

Fig. 11. HDS activity of CVD-Co/Mo/Al as a function of Co content. Some previous results [30] are also presented for comparison. ○, CVD-Co/Mo/Al(calc.); □, CVD-Co/Mo/Al(calc, NTA); ●, CVD-Co/Mo/Al (uncalc.); ⊕ CVD-Co/Mo/Al(uncalc.) corrected for the Co content of Co_9S_8 clusters; ■, CVD-Co/Mo/Al(uncalc., NTA); ⊞, CVD-Co/Mo/Al (uncalc., NTA) corrected for the Co content of Co_9S_8 clusters; △, CVD-Co/Mo/Al_2O_3 [30]; ▽, CVD-Co/Mo/TiO_2 [30]; ▼, CVD-Co/Mo/ZrO_2 [30]; ◇, CVD-Co/Mo/SiO_2 [30].

with or without NTA addition were far below the proportional line. CVD-Co/Mo/Al(calc., NTA) showed an HDS activity slightly higher than that for CoMoS(I). The activities of the uncalcined catalysts are plotted in Fig. 11 against the Co content corrected for Co sulfide clusters (Table 3). The uncalcined catalyst in the absence of NTA shifted onto the line, showing the formation of CoMoS(I), whereas CVD-Co/Mo/Al(uncalc,, NTA) exhibited an activity slightly higher than that for CoMoS(I). It is concluded that the addition of NTA reduces the edge dispersion of the resulting MoS_2 particles, while the calcination enhances the edge dispersion of MoS_2 particles irrespective of NTA addition. The addition of NTA hinders the reaction of Mo oxides and basic surface hydroxyl groups because of the formation of agglomerated Mo anion species [35,36] and, to a lesser extent, MoO_4^{2-}-NTA complex formation [43,44] and, in consequence, reduces the edge dispersion of MoS_2 particles. The effect of NTA addition remains even after the calcination at 773 K. It has been claimed [15,18] that CoMoS(I) is formed by edge decoration of MoS_2 single slabs, while CoMoS(II) by edge decoration of stacked MoS_2 slabs. Other workers [17,18,45] have reported that the presence of NTA tends to develop stacking of MoS_2 slabs to form CoMoS(II). However, the present TEM observations in Fig. 7 seems to be in conflict with these observations. The difference may result from different pH of the impregnation solutions. It is proposed that CoMoS(II) is also formed when the interactions between MoS_2 particles and support are reduced. Actually, it has been reported by Bouwens et al. [45] that Co–Mo/C catalysts are of CoMoS(II) type regardless of a single slab structure.

Table 4
Effects of calcination and NTA addition on the HDS activity of CoMo/Al[a] prepared by a coimpregnation technique

Preparation[b]	Activity[c] of CoMo/Al	Activity[c] of CVD-Co/CoMo/Al	Co content[d] (wt%)	Activity ratio[e]	Activity ratio[f]
Uncalc.	152	274	5.61	0.55	0.87
Calc.	182	305	5.45	0.60	0.86
Uncalc. + NTA	162	308	6.55	0.53	0.96
Calc. + NTA	207	350	5.36	0.59	0.98

[a] Co content, 2.0 wt%; Mo content, 9.1 wt%; Al_2O_3, JRC-ALO-4.
[b] Calc., calcined at 773 K and uncalc., dried but not calcined.
[c] 10^{-5} mol g^{-1} h^{-1}.
[d] Co content of CVD-Co/CoMo/Al.
[e] (Activity of CoMo/Al)/(activity of CVD-Co/CoMo/Al).
[f] (Activity of CVD-Co/CoMo/Al)/(activity of CVD-Co/Mo/Al).

3.3. Effects of calcination and NTA addition on the preparation of CoMo/Al_2O_3

Table 4 shows the HDS activity of CoMo/Al (Co/Mo = 0.36) prepared by a coimpregnation technique. It is apparent that the activity ranges from 152 to 207 × 10^{-5} mol h^{-1} g^{-1}, depending on the calcination and NTA addition. CoMo/Al(calc., NTA) showed the highest activity, whereas CoMo/Al(uncalc.) in the absence of NTA exhibited the lowest one. Irrespective of the calcination, the addition of NTA to the Co–Mo impregnation solution increased the catalytic activity of CoMo/Al, in agreement with other workers [17,18,45,46]. The calcination prior to sulfidation also gave favorable effects on the activity regardless of NTA addition. However, Shimizu et al. [46] reported detrimental effects of calcination on the activity of NTA-modified Co–Mo/Al_2O_3 for the HDS of benzothiophene at 1 MPa.

The HDS activity of CVD-Co/CoMo/Al is summarized in Table 4. The addition of Co significantly increased the activity. Taking into consideration the findings that the present CVD technique fills the vacant edge sites of MoS_2 particles with Co and thus gives the maximum activity [30], the ratio of the activity of CoMo/Al to that of CVD-Co/CoMo/Al provides the fraction of MoS_2 edge sites decorated with Co in CoMo/Al. The ratios are shown in Table 4. With CoMo/Al at Co/Mo = 0.36, only 53–60% of the possible edge sites of MoS_2 particles is occupied by Co to form CoMoS phases. The coverage of Co on MoS_2 edge sites was not increased by the addition of NTA and slightly increased by calcination in the present preparations.

The activity ratio of CVD-Co/CoMo/Al to that of the corresponding CVD-Co/Mo/Al in Table 3 suggests the effects of Co in the coimpregnation solution on the dispersion and stacking of MoS_2 slabs. The ratio is summarized in the last column of Table 4. The catalysts prepared in the absence of NTA obviously show considerably lower activities than CVD-Co/Mo/Al, whereas CVD-Co/CoMo/Al(NTA) catalysts show essentially identical activities with CVD-Co/Mo/Al(NTA) catalysts. The findings indicate that the edge dispersion of MoS_2 particles in CoMo/Al is consid-

erably decreased by the coimpregnation technique in the absence of NTA, possibly as a result of modification of the acid–base properties of the Al_2O_3 surface by Co and/or the formation of Co–Mo mixed oxides. In the presence of NTA, however, most of the Co^{2+} ions form Co^{2+}-NTA complexes [43,44], thus reducing the interactions of Co with the Al_2O_3 surface and/or with Mo species. Accordingly, the detrimental effects of the coexisting Co ions on the dispersion of Mo are reduced by the Co^{2+}-NTA complex formation.

3.4. Effects of Co precursor and calcination on the catalytic activity of double impregnation CoMo/Al_2O_3 catalysts

Finally, the effects of Co precursor and calcination were studied for the CoMo/Al catalysts (Co/Mo = 0.48) prepared by a conventional double impregnation technique. A precalcined MoO_3/Al_2O_3 was impregnated with an aqueous solution of Co salt, followed by drying. An aliquot of the sample was calcined at 773 K. Table 5 presents the HDS activity of CoMo/Al catalysts thus prepared. The calcined catalyst prepared by use of $Co(NO_3)_2$ showed the highest activity, while the uncalcined catalyst from $Co(CH_3COO)_2$ the lowest one. An activity difference more than 20% was generated by the catalyst preparation method.

CoMo/Al was exposed to a vapor of $Co(CO)_3NO$ and sulfided again to prepare CVD-Co/CoMo/Al. The HDS activity of the impregnation catalyst was considerably increased by the addition of Co (by 15–40%, depending on the preparation). The activity of CVD-Co/CoMo/Al is summarized in Table 5. It is worthy of note that the CVD-Co/CoMo/Al shows essentially the identical activity regardless of the calcination and Co precursor. This may be explained by assuming that the preexisting Mo oxide phases are not modified very much by the subsequent addition of Co and calcination, resulting in the formation of almost identical dispersion and morphology of MoS_2 particles.

Taking into consideration the finding that the maximum Co coverage on the MoS_2 edge sites is attained by the CVD technique [30], the Co coverage can be estimated for CoMo/Al from the activity ratio in Table 5, (activity of CoMo/Al)/(activity of CVD-Co/CoMo/Al). In the case of the uncalcined catalysts, the Co coverage of CoMo/Al is relatively low (71 and 77%), suggesting that their low activity is simply due to a lower degree of edge decoration. The calcination considerably increased the coverage of Co as observed for the coimpregnation catalysts in Table 4. This may be due to increased interaction strength of Co with the support surface during the calcination and, accordingly, an increased dispersion (for instant, surface Co^{2+}_{oct} species as reported by several groups [1,18,41,47]). It is surmised that the former effect increases the sulfidation temperature of Co and then the fraction of Co on MoS_2 edge sites. The preferable effect of nitrate to acetate may be a consequence of higher stability or inertness of the acetate complex toward the interaction with MoO_3/Al_2O_3. It is suggested that the present preparation technique of the model catalysts predicts the potential maximum activities attainable when the edge sites of MoS_2 particles are fully covered by Co, that is, when the amount of CoMoS phases is maximized. Furthermore, the present preparation technique using $Co(CO)_3NO$ provides a unique characterization method to evaluate the Co coverage on the edge sites of MoS_2 particles for supported Co–Mo sulfide catalysts.

Table 5
Effects of Co precursor and calcination on the HDS activity of CoMo/Al[a] prepared by a double impregnation technique

Preparation		Activity[c] of	Activity[c] of	Activity
Precursor	Calcination[b]	CoMo/Al	CVD-Co/CoMo/Al	ratio[d]
Co nitrate	Uncalc.	257	335	0.77
	Calc.	294	337	0.87
Co acetate	Uncalc.	232	326	0.71
	Calc.	269	336	0.80

[a] Co content, 2.7 wt%; Mo content, 9.1 wt%; Al_2O_3, JRC-ALO-6.
[b] Calc., calcined at 773 K and uncalc., dried but not calcined after the impregnation of Co.
[c] 10^{-5} mol g^{-1} h^{-1}.
[d] (Activity of CoMo/Al)/(activity of CVD-Co/CoMo/Al).

4. Conclusions

Summarizing the present study on the preparation of Co–Mo model sulfide catalysts and their application to the effects of the preparation of HDS catalysts, the conclusions are as follows:

1. Alumina-supported Co–Mo model sulfide catalysts, in which CoMoS phases are exclusively formed, are prepared by decorating presulfided Mo/Al_2O_3 with $Co(CO)_3NO$ and subsequently sulfiding. It is required that the Mo content of Mo/Al_2O_3 exceeds a monolayer loading and that Mo/Al_2O_3 is calcined prior to the sulfidation.
2. The amount of Co forming CoMoS phases is estimated from the correlation between NO/Mo and Co/Mo ratios except for the catalysts having a predominant amount of oxysulfides.
3. The NTA addition in the preparation of Mo/Al_2O_3 prevents the interactions of Mo oxides and Al_2O_3 surface and, in consequence, reduces the edge dispersion of MoS_2 slabs, when pH of the impregnation solution is not adjusted.
4. The calcination of Mo/Al_2O_3 increases the dispersion of Mo sulfide phases regardless of NTA addition.
5. The effects of NTA addition to Co–Mo/Al_2O_3 coimpregnation catalysts reduce the detrimental effects of Co on the Mo oxide dispersion. The calcination increases the Co coverage on the edge sites of MoS_2 particles

in both simultaneous and sequential impregnation catalysts.

6. It is suggested that the present preparation technique of the model catalysts predicts the potential maximum activities attainable when the edge sites of MoS_2 particles are fully covered by Co.
7. With Co–Mo sulfide catalysts, the Co coverage on the edge sites of MoS_2 particles can be evaluated by the present CVD technique.

Acknowledgments

This work has been entrusted by the New Energy and Industrial Technology Development Organization under a subsidy of the Ministry of Economy, Trade, and Industry. We are grateful to Dr. T. Fujikawa and Mr. T. Ebihara (Cosmo Research Institute) for the TEM observations of the catalysts. We also express our thanks to Prof. Y. Sawada (Department of Geo-science, Shimane University) for providing us the opportunity to use the XRF apparatus.

References

[1] H. Topsøe, B.S. Clausen, F.E. Massoth, in: J.R. Anderson, M. Boudard (Eds.), Catalysis-Science and Technology, Vol. 11, Springer, Berlin, 1996.
[2] K. Kabe, A. Ishihara, W. Qian, Hydrodesulfurization and Hydrodenitrogenation, Kodansha, Tokyo, 1999.
[3] H. Topsøe, B.S. Clausen, Catal. Rev.-Sci. Eng. 26 (1984) 395.
[4] H. Topsøe, B.S. Clausen, N. Topsøe, E. Pederson, Ind. Eng. Chem. Fundam. 25 (1986) 25.
[5] R.R. Chianelli, Catal. Rev.-Sci. Eng. 26 (1984) 361.
[6] R. Prins, V.H.J. de Beer, G.A. Somorjai, Catal. Rev.-Sci. Eng. 31 (1989) 1.
[7] R.R. Chianelli, M. Daage, M.J. Ledoux, Adv. Catal. 40 (1994) 177.
[8] A.N. Startsev, Catal. Rev.-Sci. Eng. 37 (1995) 353.
[9] D.D. Whitehurst, T. Isoda, I. Mochida, Adv. Catal. 42 (1998) 345.
[10] M. Breysse, J.L. Portefaix, M. Vrinat, Catal. Today 10 (1991) 489.
[11] B.S. Clausen, S. Mørup, H. Topsøe, R. Candia, J. Phys. Colloq. 37 (1976) C6-249.
[12] H. Topsøe, B.S. Clausen, R. Candia, C. Wivel, S. Mørup, J. Catal. 68 (1981) 433.
[13] C. Wivel, R. Candia, B.S. Clausen, M. Mørup, H. Topsøe, J. Catal. 68 (1982) 453.
[14] H. Topsøe, B.S. Clausen, R. Candia, C. Wivel, S. Mørup, Bull. Soc. Chim. Belg. 90 (1981) 1189.
[15] R. Candia, O. Sørensen, J. Villadsen, N. Topsøe, B.S. Clausen, H. Topsøe, Bull. Soc. Chim. Belg. 93 (1984) 763.
[16] M.S. Thomson, European Patent 0181035, 1986.
[17] J.A.R. van Veen, E. Gerkema, A.M. van der Kraan, A. Knoester, J. Chem. Soc. Chem. Commun. (1987) 1684.
[18] J.A.R. van Veen, E. Gerkema, A.M. van der Kraan, P.A.J.M. Hendriks, H. Beens, J. Catal. 133 (1992) 112.
[19] S.P.A. Louwen, R. Prins, J. Catal. 133 (1992) 94.
[20] L. Medici, R. Prins, J. Catal. 163 (1996) 94.
[21] J.A.R. van Veen, H.A. Colijn, R.A.J.M. Hendriks, J.A. van Welsenes, Fuel Proc. Technol. 35 (1993) 137.
[22] F. Maugé, A. Vallet, J. Bachelier, J.C. Duchet, J.C. Lavelley, Catal. Lett. 2 (1989) 57.
[23] F. Maugé, A. Vallet, J. Bachelier, J.C. Duchet, J.C. Lavelley, J. Catal. 162 (1996) 88.
[24] M. Angulo, F. Maugé, J.C. Duchet, J.C. Lavalley, Bull. Soc. Chim. Bell. 96 (1987) 925.
[25] T.R. Halbert, T. Ho, E.I. Stiefel, R.R. Chianelli, M. Daage, J. Catal. 130 (1991) 116.
[26] Y. Okamoto, M. Odawara, H. Onimatsu, T. Imanaka, Ind. Eng. Chem. Res. 34 (1995) 3707.
[27] Y. Okamoto, H. Katsuyama, Stud. Surf. Sci. Catal. 101 (1996) 503.
[28] Y. Okamoto, H. Katsuyama, AIChE J. 43 (1997) 2809.
[29] Y. Okamoto, H. Okamoto, T. Kubota, H. Kobayashi, O. Terasaki, J. Phys. Chem. B 103 (1999) 7160.
[30] Y. Okamoto, K. Ochiai, M. Kawano, K. Kobayashi, T. Kubota, Appl. Catal. A 226 (2002) 115.
[31] J.L. Roustan, Y. Lijour, B.A. Morrow, Inorg. Chem. 26 (1987) 2509.
[32] T. Fujikawa, K. Idei, K. Ohki, H. Mizuguchi, K. Usui, Appl. Catal. A 205 (2001) 71.
[33] Y. Okamoto, A. Maezawa, T. Imanaka, J. Catal. 120 (1989) 29.
[34] F.E. Massoth, Adv. Catal. 27 (1978) 265.
[35] W.K. Hall, in: R. Vanselow, R. Howe (Eds.), Chemistry and Physics of Solid Surfaces IV, Springer, Berlin, 1986, p. 73.
[36] W.K. Hall, in: H.F. Barry, P.C.H. Mitchell (Eds.), Proceedings of the Climax Fourth International Congress on the Chemistry and Uses of Molybdenum, Climax Molybdenum, Ann Arbor, MI, 1982, p. 224.
[37] Y. Okamoto, T. Imanaka, J. Phys. Chem. 92 (1988) 7102.
[38] H. Knözinger, P. Ratnasamy, Catal. Rev.-Sci. Eng. 17 (1978) 31.
[39] C.P. Li, D.M. Hercules, J. Phys. Chem. 88 (1984) 456.
[40] Y. Okamoto, Y. Katoh, Y. Mori, T. Imanaka, S. Teranishi, J. Catal. 70 (1981) 445.
[41] N.Y. Topsøe, H. Topsøe, J. Catal. 77 (1982) 293.
[42] E. Payen, R. Hubaut, S. Kasztelan, O. Pulet, J. Grimblot, J. Catal. 147 (1994) 123.
[43] L. Medici, R. Prins, J. Catal. 163 (1996) 28.
[44] K. Inamura, K. Uchikawa, S. Matsuda, Y. Akai, Appl. Surf. Sci. 121/122 (1997) 468.
[45] S.M.A.M. Bouwens, F.B.M. van Zon, M.P. van Dijik, A.M. van der Kraan, V.H.J. de Beer, J.A.R. van Veen, D.C. Koningsberger, J. Catal. 146 (1994) 375.
[46] H. Shimizu, S. Kasahara, T. Kiyohara, M. Kawahara, M. Yamada, Sekiyu Gakkai-shi 38 (1995) 384.
[47] C. Wivel, B.S. Clause, R. Candia, H. Topsøe, J. Catal. 87 (1984) 497.